

Electronic Supplementary Information

## Exploring Crown-Ether Functionalization on the Stabilization of Hexavalent Neptunium.

Mikaela M. Pynch, James M. Williams, and Tori Z. Forbes

### Synthesis

*Synthesis: **WARNING:** Neptunium-237 is a highly radioactive alpha emitter and as such is considered a health risk. Research involving this isotope is restricted to specialized laboratories and handled under appropriate regulatory controls and safe working practices.* The reagents dicyclohexano-18-crown-6 (DCH18C6), (C<sub>12</sub>H<sub>24</sub>O<sub>6</sub>, Acros Organics), potassium chloride (KCl, Fisher Scientific), sodium chloride (NaCl, Fisher Scientific), and methanol (CH<sub>3</sub>OH, Sigma Aldrich) were used as received. Approximately 200 mg of <sup>237</sup>Np was reprocessed from previous synthetic experiments, precipitated using saturated NaOH, and purified by a cation exchange column containing Dowex-50-X8 resin. Potassium bromate was added to the solution to create the Np(VI) stock solution. The resulting neptunyl (V or VI) solution was again precipitated with sodium hydroxide, the solid was washed with ultrapure H<sub>2</sub>O, and dissolved in 1.0 M HCl. The final concentration of <sup>237</sup>Np in each stock solution was determined using a Packard Tri-Carb Liquid Scintillation Counter. The oxidation state of the stock solution was confirmed with Raman spectroscopy (Figures S1 and S2).

**Compound 1:** (K(DCH18C6)<sub>2</sub>[NpO<sub>2</sub>Cl<sub>4</sub>]<sub>2</sub>) was synthesized by adding 300 μL of a 65 mM Np(VI) stock solution and 400 μL of a 100 mM DCH18C6 methanol solution to a glass vial. DCH18C6 is only sparingly soluble in aqueous solution, so we utilized methanol for the solvent. The vial was allowed to sit uncapped for three days. At which time, yellow crystals formed on the bottom of the vial and LSC of the remaining mother liquor indicated that the solid formed in 90% yield. Potassium was not added to the solution, but is present as a contaminant phase from the potassium bromate oxidation. Additional experiments with KCl added to the solution also yielded crystals of **1**.

**Compound 2:** Crystallization of (Na(DCH18C6)<sub>2</sub>[NpO<sub>2</sub>Cl<sub>4</sub>]<sub>2</sub>) occurred in a similar fashion to compound **1**. The Np(VI) stock solution (200 μL of 65 mM) was added to a glass vial containing 680 of the 100 mM DCH18C6 stock and 170 μL of a 100 mM NaCl solution. Again yellow crystals formed in 90% yields at the bottom of the vial after three days of room temperature evaporation.

**Additional Crystallization experiments:** Attempts to crystallize the Np(V) analogue of compounds **1** and **2** were unsuccessful. The unsuccessful synthesis contained 200 μL of 65 mM Np(V) stock solution and 680 μL of a 100 mM DCH18C6 solution and yielded clear salt crystals with an amorphous green solid. We also attempted the synthesis with a mixed Np(V)/Np(VI) solution which was confirmed via Raman spectroscopy (Fig. S3), using the same procedure that led to compound **1**. The mixed valent solution was created by combining 100 μL of a 65 mM Np(V)

stock with 100  $\mu\text{L}$  of a 85 mM. Yellow crystals formed at the bottom of the vial after three days of room temperature evaporation, leaving behind an emerald green solution (Fig. S4).

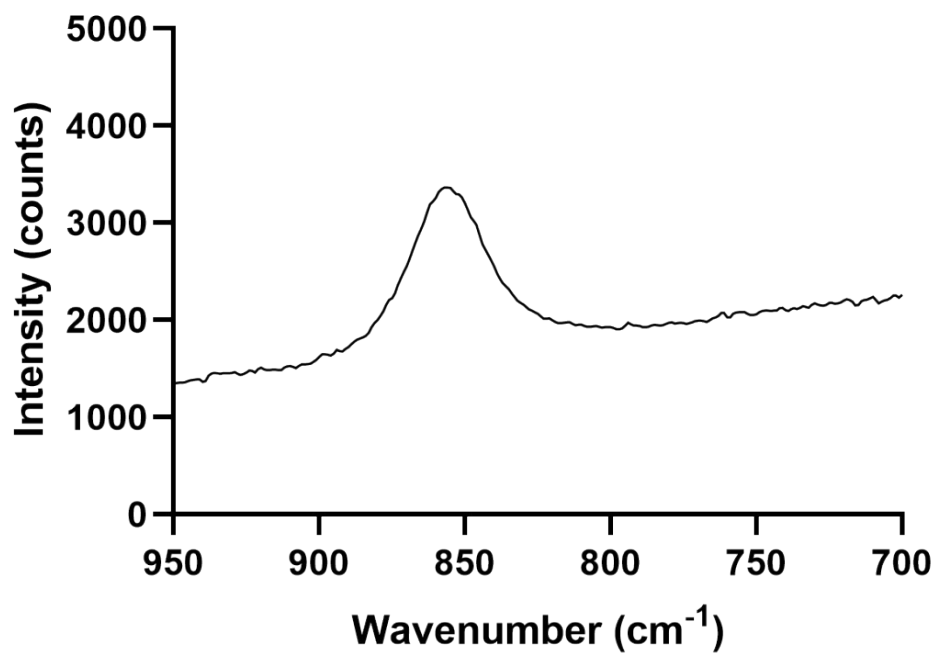


**Figure S1.** Raman spectrum of the initial Np(VI) stock solution used for all experiments.

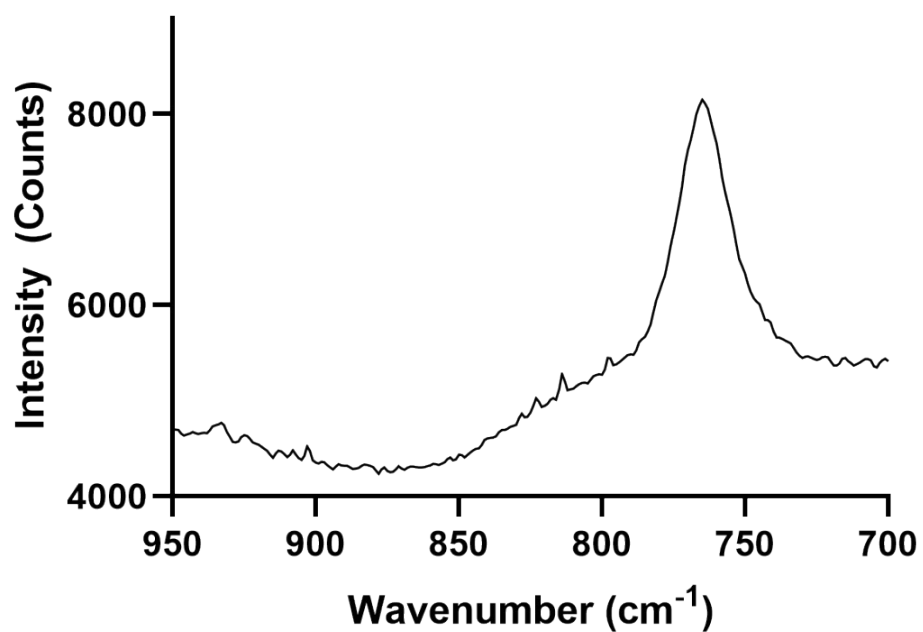


**Figure S2.** Raman spectrum of the Np(V) stock solution used for additional experiments.

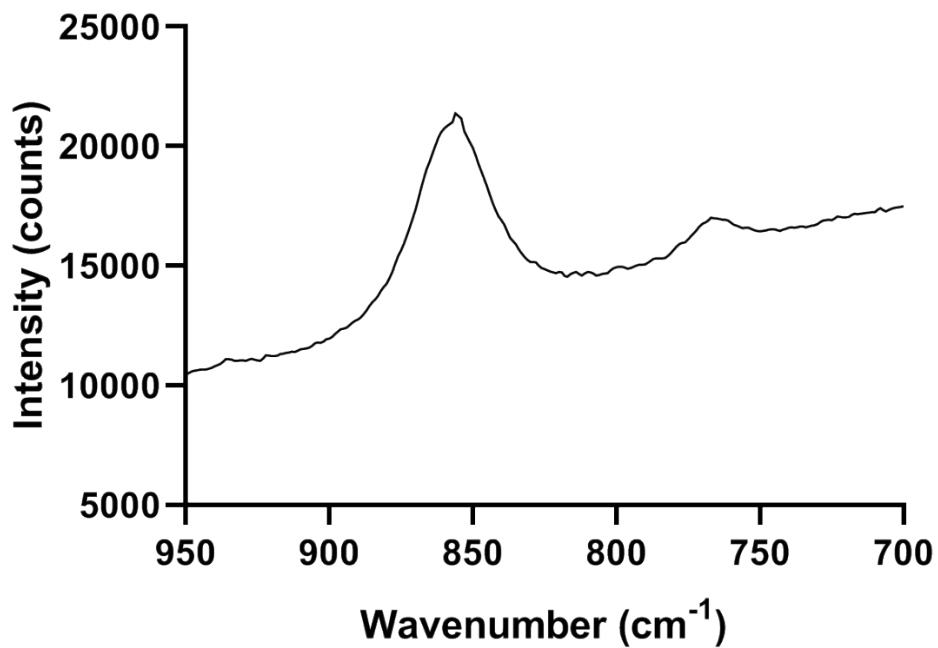


**Figure S3.** Raman spectrum of the mixed Np(V)/Np(VI) solution that was utilized for the synthetic procedure.

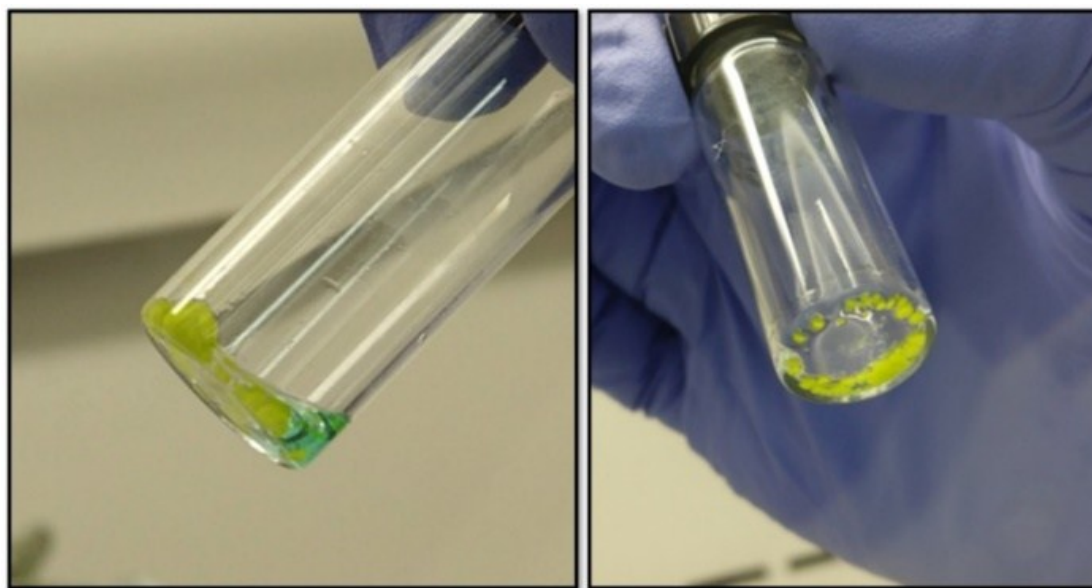


**Figure S4.** Images displaying the crystallization of **1** from a mixed valent Np(VI)/Np(V) solution. The yellow solid is the Np(VI)DCH-18C6 compound, while the remaining mother-liquor retains an emerald green colour associated with Np(V).

### Structural Characterization using Single Crystal X-ray Diffraction

Single crystals of **1** and **2** were isolated from their mother liquor and mounted on a MiTeGen MicroMount with NVH immersion oil (Cargille Labs). Frames were collected on a Bruker D8 Quest single crystal X-ray diffractometer equipped with a microfocus beam (Mo K $\alpha$ ;  $\lambda = 0.71073 \text{ \AA}$ ) and Oxford Systems low temperature cryosystem operating at 100 K. Data were collected with the Bruker APEX3 software package<sup>1</sup> and peak intensities were corrected for (Lorentz, polarization, background effects, and absorption). The structure solution was determined by intrinsic phasing methods and refined on the basis of  $F^2$  for all unique data using the SHELXTL version 5 series of programs.<sup>2</sup> Np atoms were located by direct methods and the C, O, Na, K, and Cl atoms were found and modeled from the difference Fourier maps. Initial space group refinements suggested a C centered lattice for **2**, but resulted in 212 inconsistent equivalents, a high  $R_{int}$  value (13%), and significant disorder of the crown ether molecule. A primitive Bravais lattice was identified using the CELLNOW software<sup>3</sup> and resulted in the final  $P2_1/c$  space group assignment. This space group choice eliminated the structural disorder and modeling issues. Disorder of several C atoms associated with the dicyclohexano-18-crown-6 (DCH-18C6) molecule was observed in both **1** and **2**. These atoms could not be refined anisotropically due to unrealistic thermal ellipsoids even when modeled as split sites with partial occupancy. In addition, the K atoms in **1** possess structural

disorder and were also modeled over several crystalline positions with refined occupancies. Hydrogen atoms associated with the DCH-18C6 ligands were fixed using a riding model when possible. The crystallographic information files can be found on the Cambridge Structural Database by requesting numbers 1921583 and 1921584.

**Table S1.** Select crystallographic information for **1** and **2**.

	<b>1</b>	<b>2</b>
Empirical formula	C <sub>40</sub> H <sub>72</sub> Cl <sub>4</sub> K <sub>2</sub> NpO <sub>14</sub>	C <sub>40</sub> H <sub>72</sub> Cl <sub>4</sub> Na <sub>2</sub> NpO <sub>14</sub>
Formula weight	1233.71	1201.50
Space group	<i>P2<sub>1</sub>/c</i>	<i>P2<sub>1</sub>/c</i>
<i>a</i>	14.446(1)	8.991(10)
<i>b</i>	20.131(2)	27.0388(2)
<i>c</i>	25.473(2)	10.6369(6)
$\alpha$	90	90
$\beta$	91.278(3)	92.82(7)
$\gamma$	90	90
<i>V</i>	7406.3(11)	2583.7(4)
<i>Z</i>	2	2
$\rho$ (g/cm <sup>3</sup> )	1.647	1.525
$\mu$ (mm <sup>-1</sup> )	2.549	2.292
F(000)	3682	1182
$\theta$ range for data collection (°)	2.176 to 25.470	2.268 to 26.372
Limiting indices	-17 < <i>h</i> < 17 -24 < <i>k</i> < 24 -30 < <i>l</i> < 30	-11 < <i>h</i> < 11 -33 < <i>k</i> < 33 -11 < <i>l</i> < 11
Reflections collected / unique	123080 / 13675	95230 / 5276
<i>R</i> <sub>int</sub>	0.0758	0.0699
Data / restraints / parameters	13675 / 0 / 813	5276 / 0 / 273
GOF on <i>F</i> <sup>2</sup>	1.130	1.106
Final <i>R</i> indices	<i>R</i> <sub>1</sub> = 0.0512	<i>R</i> <sub>1</sub> = 0.0397
[ <i>I</i> > 2 $\sigma$ ( <i>I</i> )]	<i>wR</i> <sub>2</sub> = 0.1086	<i>wR</i> <sub>2</sub> = 0.0877
<i>R</i> indices (all data)	<i>R</i> <sub>1</sub> = 0.0741 <i>wR</i> <sub>2</sub> = 0.1179	<i>R</i> <sub>1</sub> = 0.0623 <i>wR</i> <sub>2</sub> = 0.0950
Largest diff. peak and hole	1.516 and -1.810	0.697 and -0.787

**Table S2.** Select Bond Distances (Å) and Angles (°) for **1** and **2**.

<b>1</b>				<b>2</b>	
Np(1)-O(1)	1.738(6)	Np(1)-O(3)	1.744(4)	Np(1)-O(1)	1.774(4)
Np(1)-O(2)	1.734(5)	Np(1)-O(3)	1.744(4)	Np(1)-O(1)	1.774(4)
Np(1)-Cl(2)	2.645(2)	Np(1)-Cl(5)	2.651(2)	Np(1)-Cl(1)	2.612(2)
Np(1)-Cl(1)	2.646(2)	Np(1)-Cl(5)	2.651(2)	Np(1)-Cl(1)	2.612(2)
Np(1)-Cl(3)	2.647(2)	Np(1)-Cl(6)	2.659(2)	Np(1)-Cl(2)	2.680(2)
Np(1)-Cl(4)	2.665(2)	Np(1)-Cl(6)	2.659(2)	Np(1)-Cl(2)	2.680(2)
O(1)-Np(1)-O(1)	179.3(3)	O(3)-Np(1)-O(3)	180.0	O(1)-Np(1)-O(1)	180.0
Cl(1)-Np(1)-Cl(2)	87.80(7)	O(3)-Np(1)-Cl(5)	91.2(2)	O(1)-Np(1)-Cl(1)	89.8(1)
Cl(3)-Np(1)-Cl(4)	90.30(6)	O(3)-Np(1)-Cl(6)	90.2(2)	O(1)-Np(1)-Cl(2)	90.2(1)

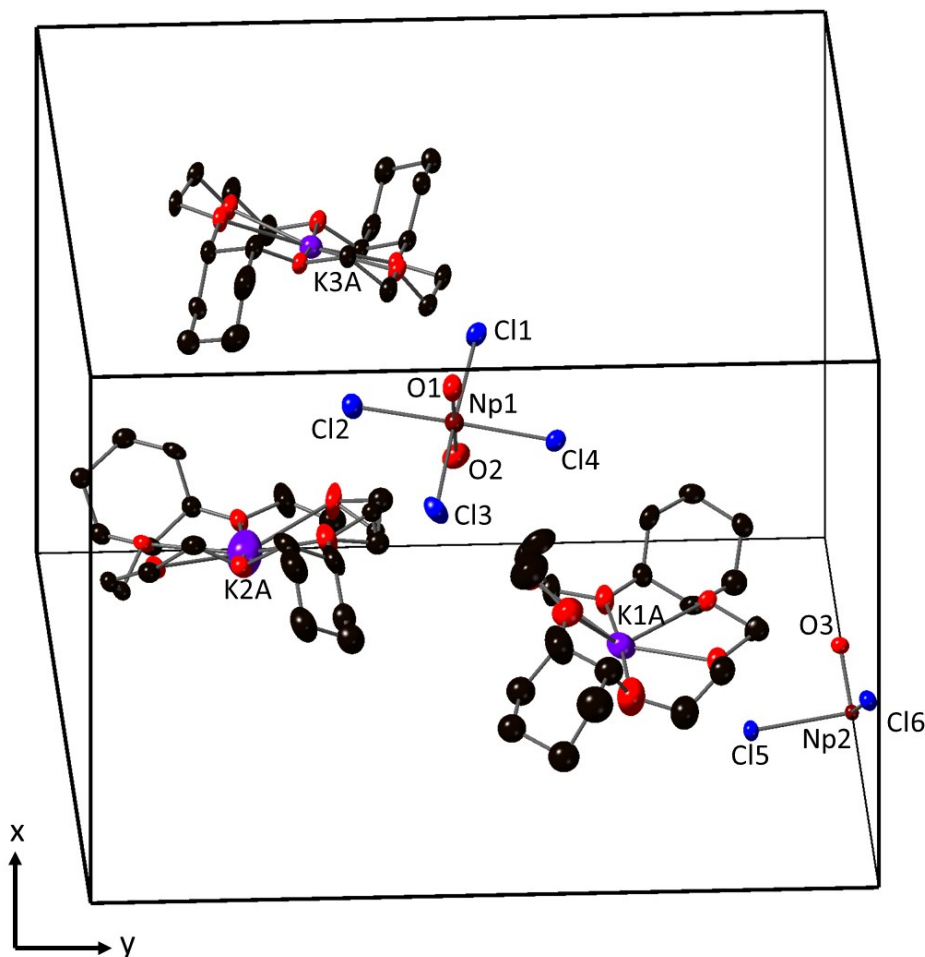


**Figure S5.** Asymmetric unit of **1** depicted using thermal ellipsoids (50%). Np (maroon), Cl (blue), K (purple), and neptunyl oxo (red) atoms are labeled. Atoms within the DCH-18C6 molecules (carbon (black) and oxygen atoms (red)) were not labeled and H atoms were removed for clarity.

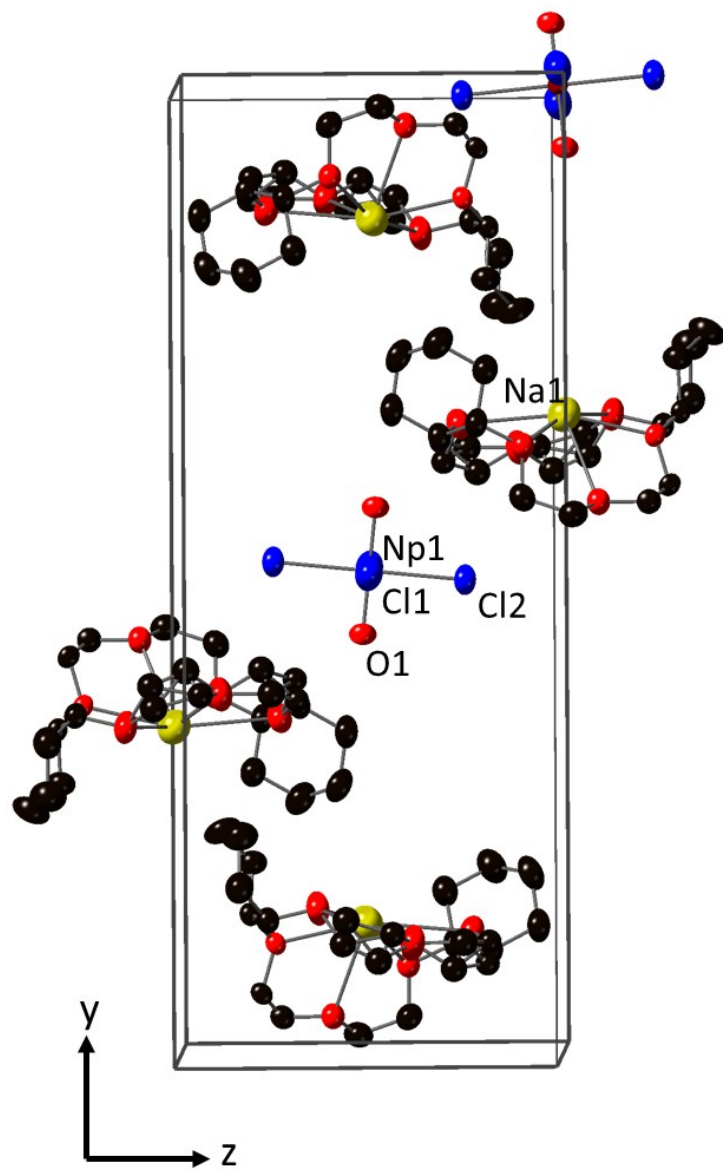


**Figure S6.** Unit cell contents of **2** depicted using thermal ellipsoids (50%). Np (maroon), Cl (blue), Na (yellow), and neptunyl oxo (red) atoms are labeled. Atoms within the DCH-18C6 molecules (carbon (black) and oxygen atoms (red)) were not labeled and H atoms were removed for clarity.



## Raman spectroscopy

To collect solid state Raman spectroscopy, crystals of compounds **1** and **2** were isolated from the mother liquor and placed on a glass slide with a small amount of NVH immersion oil. Raman spectroscopy was also used to analyze the solution phase before and after crystallization of the solid-state species in 5 mL glass Raman vials. The spectra in Figure 3 are of the following solutions: (a-green line) 200  $\mu\text{L}$  of 65 mM Np(V) stock solution and 680  $\mu\text{L}$  of 100 mM DCH18C6 in methanol, (b – red line) 300  $\mu\text{L}$  of 65 mM Np(VI) stock solution and 400  $\mu\text{L}$  of DCH18C6 in methanol, and (c – blue line) 100 mM DCH18C6 in methanol.

Both solid-state and solution phase Raman spectra were acquired on a SnRI High-Resolution Sierra 2.0 Raman spectrometer equipped with 785 nm laser energy and 2048 pixels TE-cooled CCD. Laser power was set to the maximum output value of 15 mW, giving the highest achievable spectral resolution of  $2\text{ cm}^{-1}$ . Each sample was irradiated for an integration time of 20 seconds and automatically reiterated three times in Multi-Acquisition mode. The average of the three Raman spectra acquired for a sample is reported as the final Raman spectrum. To accurately process the Raman signals observed, the background was subtracted, multiple peaks were fit using the peak analysis protocol with Gaussian functions, and all the fitting parameters converged in the OriginPro 9.1.0 (OriginLab, Northampton, MA) 64-bit software.

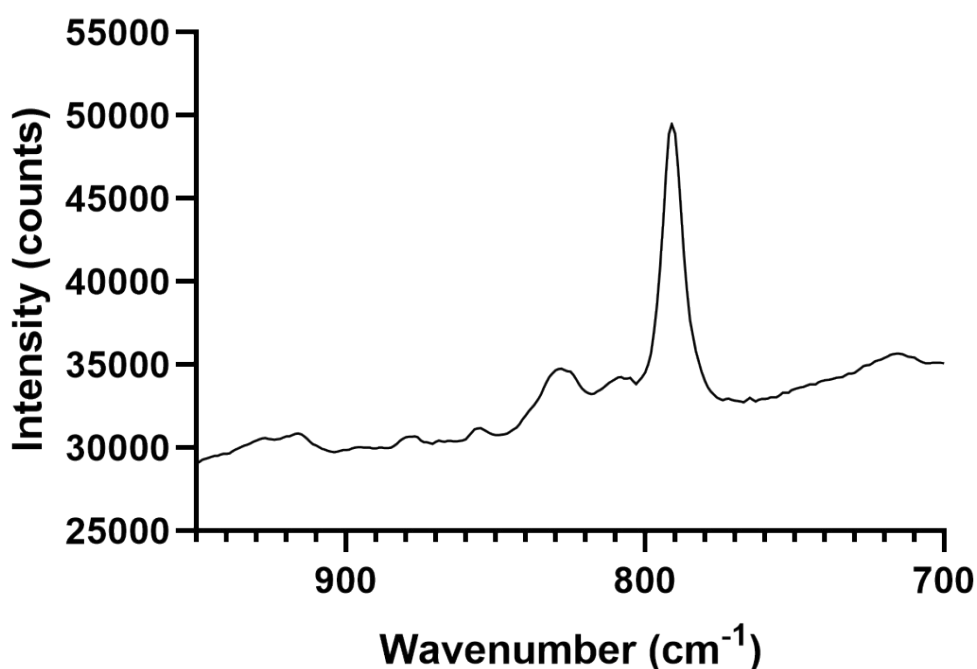


**Figure S7.** Solid state Raman spectrum of compound **1** between 700-950  $\text{cm}^{-1}$ .

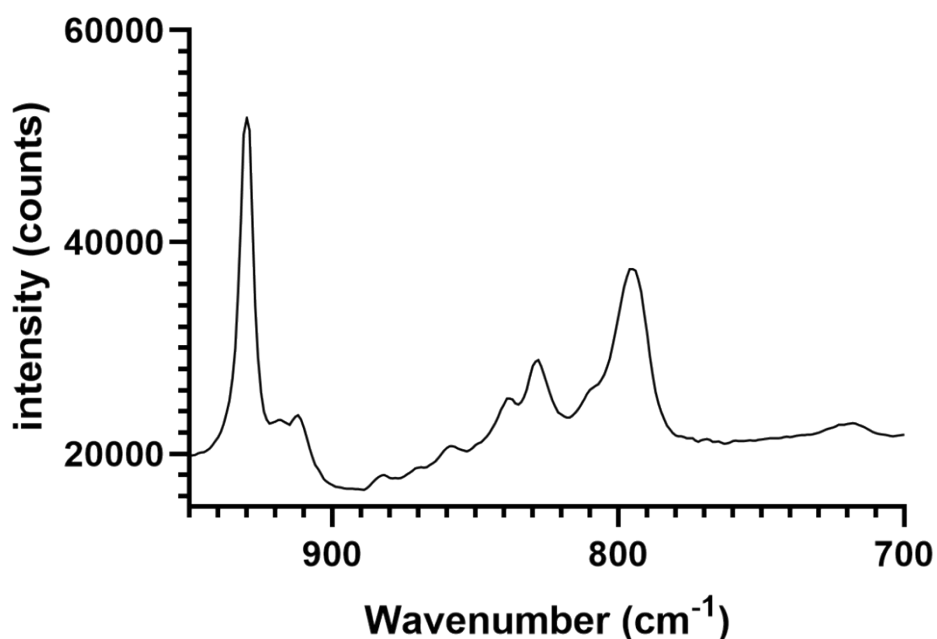


**Figure S8.** Solid state Raman spectrum of compound **2** between 700-950  $\text{cm}^{-1}$ .

**Table S3.** Bands ( $\text{cm}^{-1}$ ) present between 700-950  $\text{cm}^{-1}$  for the solid-state Raman spectra of **1** and **2**. Comparative literature values for free dicyclohexano-18C6 (DCH-18C6) in the *cis-syn-cis* and *cis-anti-cis* conformations and  $\text{Na}^+$ -encapsulated DCH-18C6 (*cis-anti-cis* isomer) are provided by Takeuchi *et al.*<sup>4</sup>

<b>1</b>	<b>2</b>	<b>Free DCH-18C6 (<i>cis-syn-cis</i>)</b>	<b>Free DCH-18C6 (<i>cis-anti-cis</i>)</b>	<b>Na-DCH-18C6 (<i>cis-anti-cis</i>)</b>
714	720	714		
793	796	783	777	794
805	802			
809	809			809
825		824	824	
830	829			
838	839	838		838
		844	845	
855	859			859
878	870	880	879	870
881	883	889	886	887
	912	904	907	905
916	919	915	914	914
928	930			923
			948	

## Semi-quantitative analysis of Np(VI) reduction using Raman spectroscopy

Raman spectroscopy was utilized to monitor the  $\text{Np(VI)O}_2^{2+}$  reduction in the presence of 18C6 and DCH-18C6 ligands. Solutions were placed in 5 mL Raman vials with an aluminum reflective cap. The initial Np(VI) DCH18C6 solution contained 300  $\mu\text{L}$  of 65 mM Np(VI) stock solution and 400  $\mu\text{L}$  of DCH18C6 in methanol. For the Np(VI)18C6 solution we used 300  $\mu\text{L}$  of a 65mM Np(VI) stock solution and added 600 microliters of a 100mM 18C6 aqueous solution. Raman spectra were collected on these samples initially (Laser power 15 MW and collection time 20 seconds with three spectra averaged for final analysis) and then after 24, 48, and 72 hours. It is important to note that there is methanol in the Np(VI) DCH18C6 and this could impact the redox behavior. However, we would expect the reduction to occur more readily in the presence of methanol than in pure water based upon previous work by Tananev<sup>5</sup> and Sessler *et al.*<sup>6</sup>

The  $\nu_1$  symmetric stretching band for neptunium is typically observed at 767  $\text{cm}^{-1}$  and 855  $\text{cm}^{-1}$  for the  $[\text{Np(V)O}_2(\text{H}_2\text{O})_5]^+$  and the  $[\text{Np(VI)O}_2(\text{H}_2\text{O})_5]^{2+}$  species, respectively. These bands were observed in the Np(V) and Np(VI) stock solutions (Figures S3 and S4). Both the 18C6 and DCH18C6 contain bands in the spectral window of interest, therefore multi-peak fitting was again utilized to assess the bands present in the solutions.

The initial Np(VI) DCH18C6 spectra contained five spectral features at 852, 837, 829, 809, and 789  $\text{cm}^{-1}$  (Fig. S9). The  $\text{Np(VI)O}_2^{2+}$  symmetric stretch can be assigned to the feature at 852  $\text{cm}^{-1}$  and the other peaks are associated with the DCH18C6 in the *cis-syn-cis* isomer. Over the course of 24 hours a band at 786  $\text{cm}^{-1}$  appears in the spectra and can be assigned to the ingrowth of the *cis-anti-cis* DCH-18C6 isomer in solution (Fig. S10).<sup>4</sup> There is no spectra feature that can be fit to a  $\nu_1$   $\text{Np(V)O}_2^+$  band, which should appear at 767  $\text{cm}^{-1}$ . Thus, we concluded that the Np(VI) species present in solution was not being reduced to Np(V) in any considerable amount.

For the Np18C6 solution, the initial spectra was successful fit with three bands (861, 836 and 810  $\text{cm}^{-1}$ ) (Fig. S11). All three bands could be assigned to the 18C6 molecule based upon previous work by Al-Kathani *et al.*<sup>7</sup> The  $\nu_1$   $\text{Np(VI)O}_2^{2+}$  symmetry stretch should be present at  $\sim 855$   $\text{cm}^{-1}$ , but this band could not be successfully included in the fit. When we attempted to include a band at  $\sim 855$   $\text{cm}^{-1}$  in our initial fit, the model failed to converge. The  $\nu_{43}$  band of the crown ether molecule at 861  $\text{cm}^{-1}$  is the strongest vibrational mode in the spectra and overlaps significantly with the neptunyl symmetric stretch. With the low concentration of the Np(VI) compared to the 18C6 molecule, there is only a small contribution of the  $\nu_1$  to the spectral feature. Therefore, we believe that the band is present but the intensity of this feature is too small to be successfully modeled. After 24 hours, an additional band at 767  $\text{cm}^{-1}$  can be observed that is assigned to the  $\nu_1$   $\text{Np(V)O}_2^+$  symmetric stretch (Fig. S11).

To further assess the extent of the Np reduction in the presence of 18C6, we utilized previous experiments<sup>8</sup> and methodology<sup>9</sup> to standardize our system. In our previous work, we titrated 18C6 into a Np(V) stock solution and assess the bands using our standard methodology. From

this we can take the intensity ratio of the  $\nu_1$   $\text{Np(V)O}_2^+$  symmetric stretch and the  $\nu_{43}$  band of the crown ether molecule at  $861\text{ cm}^{-1}$ . This can be plotted with the  $\text{Np:18C6}$  mole ratios to provide a standard curve that was fit with a linear regression ( $y = 1.68x + 0.357$ ;  $R^2 = 0.988$ ) (Fig. S13). To assess the Np reduction in our current work, we calculated the intensity ratio of the  $\nu_1$   $\text{Np(V)O}_2^+:\nu_{43}$  18C6 and then determined the difference from the original  $\text{Np(VI):18C6}$  mole ratio. The assumptions that we made for this calculation: 1) That the contribution of the  $\text{Np(VI)}$  to the intensity at  $861\text{ cm}^{-1}$  is negligible and 2) the  $\text{Np(V)}$  signal only occurs at  $767\text{ cm}^{-1}$ .

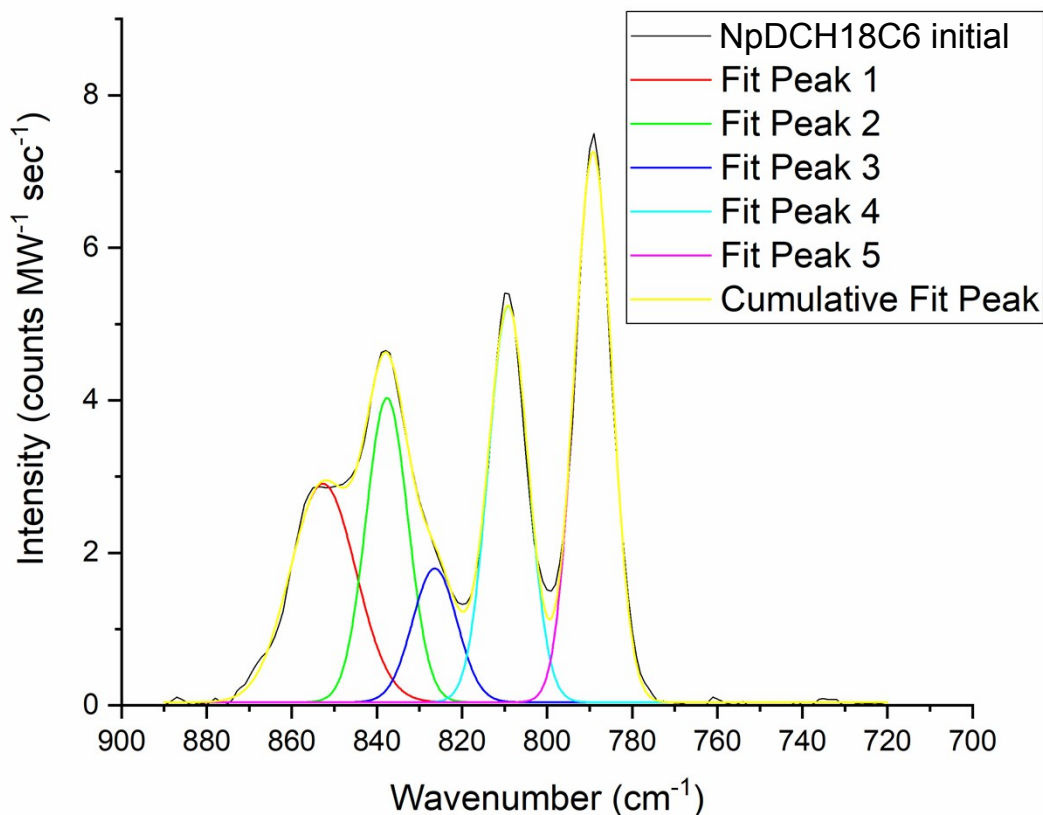


**Figure S9.** Spectral fitting of the initial  $\text{Np(VI)}$  DCH18C6 solution using the Origin software protocol.

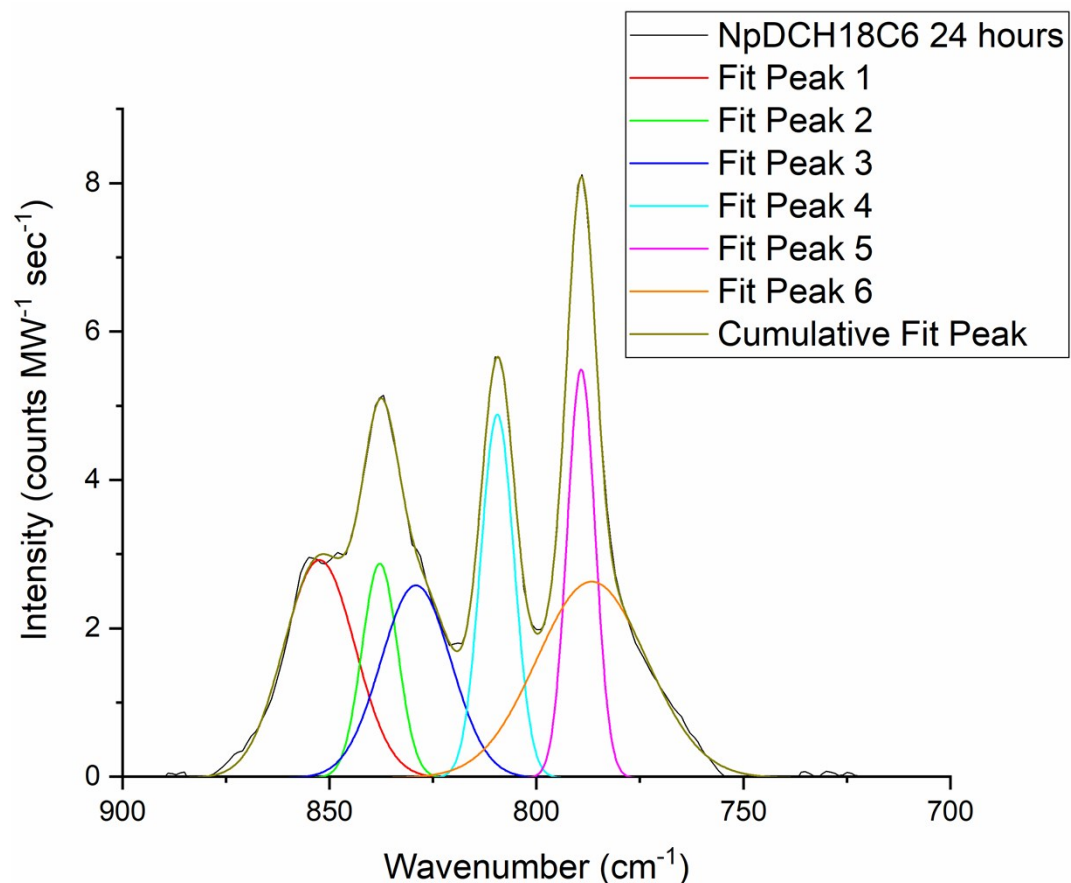


**Figure S10.** Spectral fitting of the Np(VI) DCH18C6 solution that has been aged for 24 hours,

**Table 4.** Spectral fitting data for the Np(VI) DCH18C6 solution monitored over time. Peak assignment for the DCH18C6 molecule based upon Takeuchi *et al.*<sup>4</sup>

	Peak 1	Peak 2	Peak 3	Peak 4	Peak 5	Peak 6
Assignment	$\nu_1$ (NpO <sub>2</sub> ) <sup>2+</sup>	DCH-18C6	DCH-18C6	DCH-18C6	DCH-18C6 ( <i>cis-syn-cis</i> )	DCH-18C6 ( <i>cis-anti-cis</i> )
<b>Initial</b>						
Peak centroid	852 ± 2	838 ± 2	826 ± 2	809 ± 2	789 ± 2	
FHWM	15.4 ± 0.6	9.9 ± 0.7	10 ± 1	9.4 ± 0.1	8.8 ± 0.1	
<b>24 hours</b>						
Peak centroid	852 ± 2	837 ± 2	829 ± 3	809 ± 2	789 ± 2	786 ± 2
FHWM	17.2 ± 0.7	8.6 ± 0.8	17 ± 3	8.1 ± 0.2	6.8 ± 0.1	27 ± 0.5
<b>48 hours</b>						
Peak centroid	852 ± 2	838 ± 2	828 ± 2	809 ± 2	789 ± 2	786 ± 2
FHWM	19.8 ± 0.6	8.7 ± 0.7	16 ± 3	8.5 ± 0.2	6.8 ± 0.1	26 ± 0.3
<b>72 hours</b>						
Peak centroid	852 ± 2	838 ± 2	827 ± 2	809 ± 2	789 ± 2	786 ± 2
FHWM	19.8 ± 0.9	8.9 ± 0.9	17 ± 5	8.3 ± 0.2	6.3 ± 0.1	25 ± 0.4

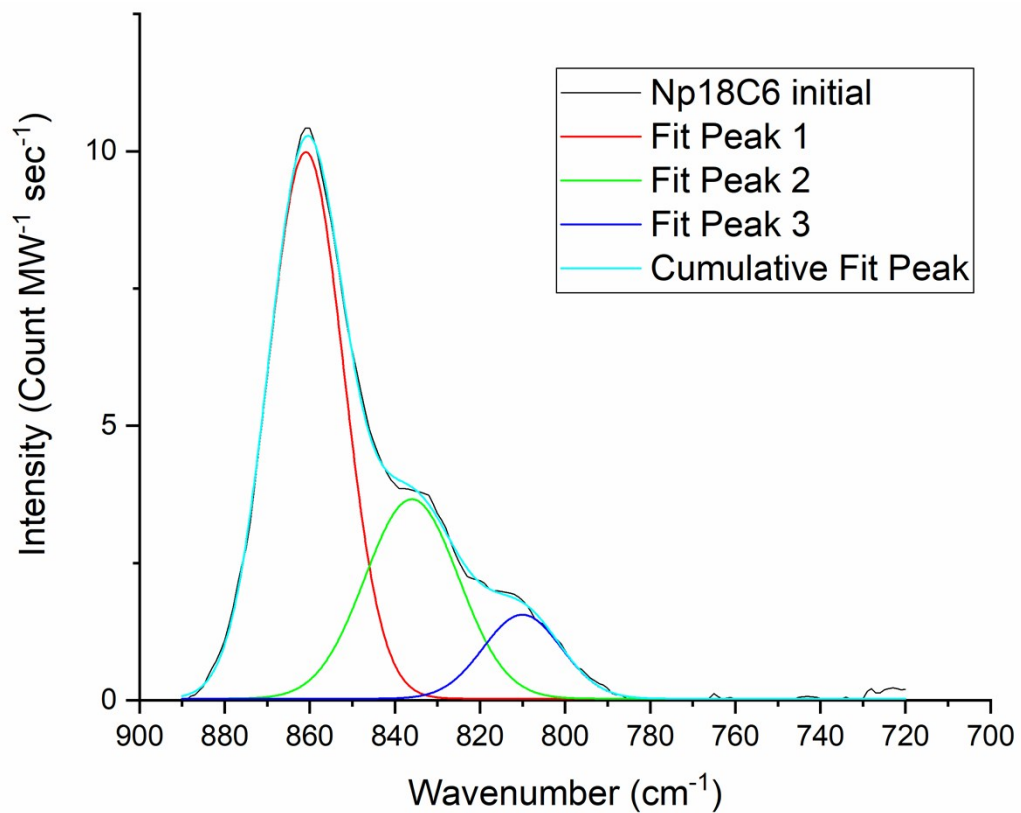


**Figure S11.** Spectral fitting of the initial Np(VI) 18C6 solution.

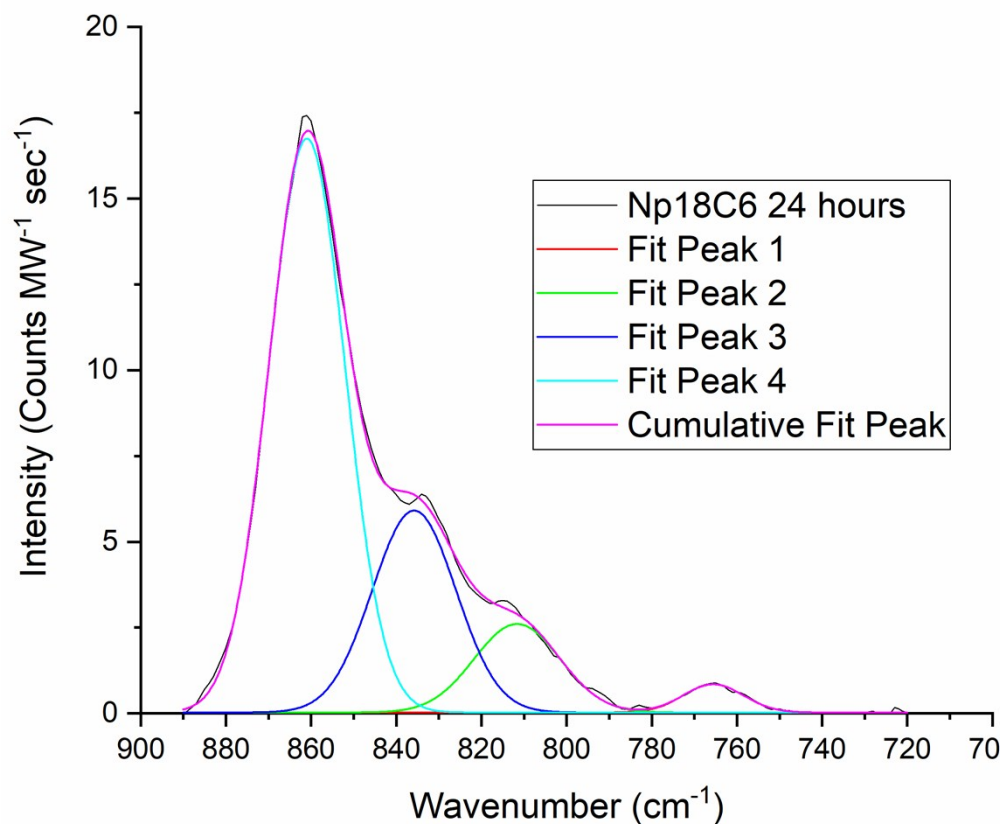


**Figure S12.** Spectral fitting of the Np(VI) 18C6 solutions, including the appearance of Np(V), which were monitored for a total 72 hours, represented is the fitting for the spectra associated with the solution after 24hrs.

**Table 5.** Spectral fitting data for the Np(VI) 18C6 solution monitored over time, including the appearance of Np(V). Peak assignment for the 18C6 molecule based upon Al-Kahtani *et al.*<sup>7</sup>

	Peak 1	Peak 2	Peak 3	Peak 4
<b>Assignment</b>	$\nu_{43}$ 18C6	$\nu_{104}$ 18C6	$\nu_{44}$ 18C6	$\nu_1$ (NpO <sub>2</sub> ) <sup>+</sup>
<b>Initial</b>				
Peak centroid	861 ± 2	836 ± 2	810 ± 2	
FHWM	17.7 ± 0.1	22 ± 1	18 ± 1	
<b>24 hours</b>				
Peak centroid	861 ± 2	836 ± 2	812 ± 2	766 ± 2
FHWM	17.9 ± 0.1	20 ± 1	20 ± 1	14 ± 1
<b>48 hours</b>				
Peak centroid	861 ± 2	835 ± 2	811 ± 2	763 ± 2
FHWM	17.6 ± 0.1	20 ± 1	17 ± 1	11.1 ± 0.9
<b>72 hours</b>				
Peak centroid	861 ± 2	836 ± 2	810 ± 3	764 ± 2
FHWM	16.8 ± 0.2	23 ± 1	18 ± 1	11.0 ± 0.7

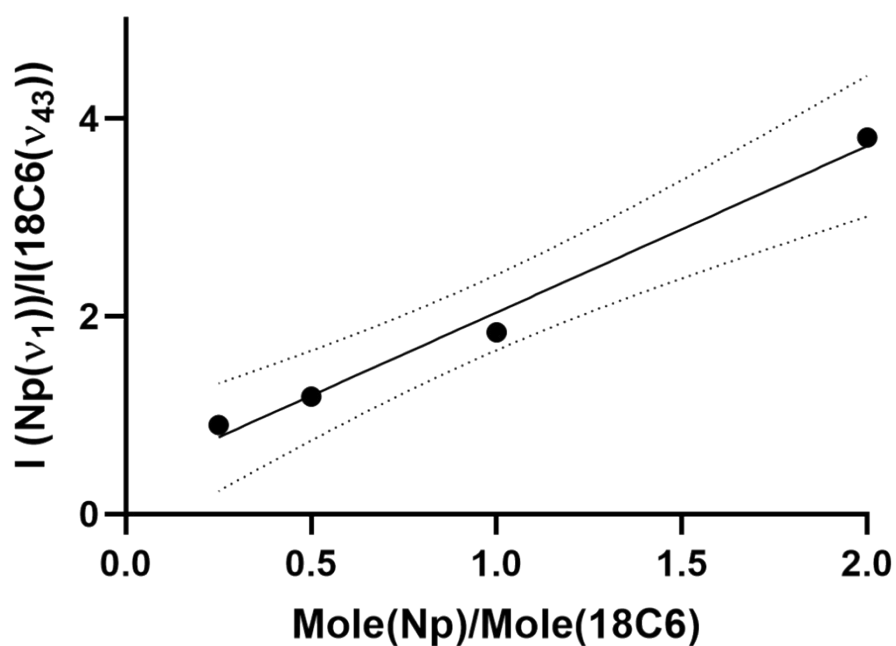


**Figure S13.** Standard curve determined from the Np(V) 18C6 titration experiment previously reported in Basile *et al.*<sup>8</sup> The filled circles represent the data points, the solid line indicates the linear regression, and the dashed lines represent the 95% confidence interval.

### References

1. G. M. Sheldrick, *Journal*, 2015.
2. G. M. Sheldrick, *Acta Crystallographica Section A: Foundations of Crystallography*, 2008, **64**, 112-122.
3. Bruker, *Journal*, 2005.
4. H. Takeuchi, T. Arai and I. Harada, *Journal of Molecular Structure*, 1990, **223**, 355-364.
5. I. G. Tananaev, *Soviet Radiochemistry*, 1990, **32**, 16-18.
6. J. L. Sessler, A. E. V. Gorden, D. Seidel, S. Hannah, V. Lynch, P. L. Gordon, R. J. Donohoe, C. D. Tait and D. W. Keogh, *Inorg. Chim. Acta*, 2002, **341**, 54-70.
7. A. A. Al-Kahtani, N. A. Al-Jallal and A. A. El-Azhary, *Spectrochimica Acta Part A: Molecular and Biomolecular Spectroscopy*, 2014, **132**, 70-83.
8. M. Basile, E. Cole and T. Z. Forbes, *Inorg. Chem.*, 2018, **57**, 6016-6028.
9. M. Basile, D. K. Unruh, K. Gojdas, E. Flores, L. Streicher and T. Z. Forbes, *Chem. Commun.*, 2015, **51**, 5306-5309.